Optically Implemented Broadband Blueshift Switch in the Terahertz Regime

Nian-Hai Shen,[1] Maria Massaouti,[2] Mutlu Gokkavas,[3] Jean-Michel Manceau,[2] Ekmel Ozbay,[3] Maria Kafesaki,[2,4]
Thomas Koschny,[1,2] Stelios Tzortzakis,[2,*] and Costas M. Soukoulis[1,2,4,†]

[1]*Ames Laboratory and Department of Physics and Astronomy, Iowa State University, Ames, Iowa 50011, USA*
[2]*Institute of Electronic Structure and Laser, FORTH, 71110 Heraklion, Crete, Greece*
[3]*Nanotechnology Research Center, and Department of Physics, Bilkent University, Bilkent, 06800 Ankara, Turkey*
[4]*Department of Materials Science and Technology, University of Crete, 71003 Heraklion, Crete, Greece*
(Received 21 September 2010; revised manuscript received 16 November 2010; published 18 January 2011)

We experimentally demonstrate, for the first time, an optically implemented blueshift tunable metamaterial in the terahertz (THz) regime. The design implies two potential resonance states, and the photoconductive semiconductor (silicon) settled in the critical region plays the role of intermediary for switching the resonator from mode 1 to mode 2. The observed tuning range of the fabricated device is as high as 26% (from 0.76 THz to 0.96 THz) through optical control to silicon. The realization of broadband blueshift tunable metamaterial offers opportunities for achieving switchable metamaterials with simultaneous redshift and blueshift tunability and cascade tunable devices. Our experimental approach is compatible with semiconductor technologies and can be used for other applications in the THz regime.

The discovery of metamaterials has greatly improved our capabilities in the manipulation of electromagnetic radiation over a large portion of the spectrum [1,2]. Many intriguing phenomena based on metamaterials, such as superlensing [3,4] and invisibility [5–8], have been proposed, and studied both theoretically and experimentally. These two ideas (invisibility and superlensing) have attracted the largest research interest recently, but unfortunately, these concepts are hard to be implemented for practical applications. However, terahertz (THz) technology has become a hopeful alternative for sensing, imaging, and applications such as amplifiers, modulators, and switches. One of the greatest obstacles in this progress is the nonexistence of materials that naturally respond well to THz radiation. One of the advantages of metamaterials for THz applications is their resonant electromagnetic response, which significantly enhances their interaction with THz radiation. Metamaterials, specifically tailored for the THz regime [9,10], where response from natural materials is somewhat rare, provide us a more robust up-to-date application of realizing various THz devices to fill the so-called "THz gap" [11–15]. It has been found that hybridized metamaterials, i.e., metamaterials with some external-source-controlled natural materials incorporated, offer us great opportunities in the construction of novel THz devices, such as dynamic notch filters [16–18], phase modulators [19,20], perfect absorbers [21–23], and frequency-agile switches [24,25]. In addition, THz radiation has many advantages, such as its nonionizing property, excellent transmission through optically opaque materials for imaging applications and the ability to detect biochemical molecules and illegal drugs. So electronic devices are pushing their boundaries to the THz regime,

where a lot of potential applications exist in different disciplines.

The key idea is to incorporate photoconductive semiconductors, as elements of metamaterial resonators, and the working frequency of the metamaterial resonator is tuned through photoexcited carrier injections. Chen *et al.* [24] experimentally achieved redshift tunability, due to a photoconductive increase in the capacitance of the metamaterial resonator. For greater flexibility in practical applications, blueshift tunable metamaterials are also of great importance and urgent necessity, especially for realizing THz devices simultaneously with redshift and blueshift tunability. However, the achievement of an optical blueshift switch is really not that easy. Chen *et al.* [24] presented two hypothetical designs targeting this goal, but they were found out of the reach of optical implementation, so they did not demonstrate experimentally the blueshift. It is found that generally for a simple inductor-capacitor resonator, the optical tuning strategy is easy for realizing an increase of capacitance but may not be efficient in changing the inductance. In this work, we have designed, fabricated, and characterized the resonant response of a blueshift tunable metamaterial with photoexcitation, which provide greater flexibility in practical applications. We show that the resonant response can be controlled using the optical or electrical approach, enabling efficient THz switches and modulators, which will be of importance for advancing numerous real world THz applications.

In order to realize a realistic blueshift tunable metamaterial, a new mechanism of a photoconductive mode switching was theoretically proposed [25]. The metamaterial was designed based on electric-field-coupled inductor-capacitor (ELC) resonators [26] and actually evolved from
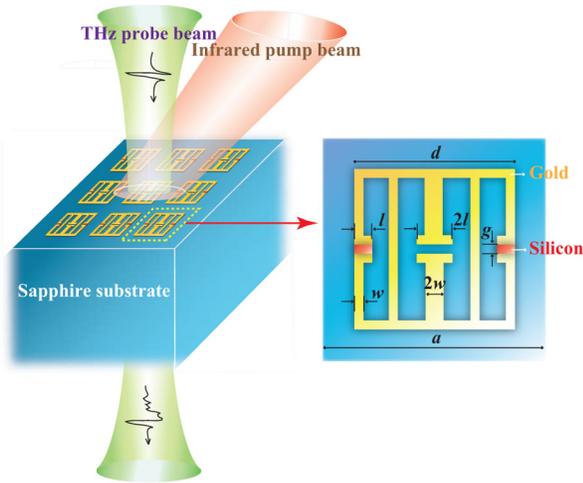
FIG. 1 (color online). Schematic of our design for a broadband blueshift tunable metamaterial device. Left: Sketch of experimental pump-probe configuration for the measurement of THz transmissions through the fabricated metamaterial device. Right: Top view to the unit cell of the designed structure showing the geometry and dimensions of the device: $a = 50$ μm, $d = 36$ μm, $l = 4$ μm, $w = 2$ μm, and $g = 2$ μm. Photoconductive silicon (red part) is put within two side gaps of the gold ELC resonator (yellow part) and the substrate is made by sapphire (blue part).

the $E1$ structure in Ref. [27]. The details of the design can be found in Fig. 1, in which photoconductive silicon is put within two side gaps of the metallic ELC resonator in each unit cell. An attentive investigation to the metallic ELC resonator may reveal that it implies two potential resonance states, while the one corresponding to the higher frequency is restrained due to the high intrinsic symmetry of the structure. Compared to the case with no pump, the silicon within the gaps of the two side paths becomes conductive through photoinjection when applying the pump, and the structure is then forced to switch from mode 1 (lower frequency) to mode 2 (higher frequency). In view of an effective circuit model, both inductance and capacitance decrease when the pump is applied, and an all-optical blueshift switching effect is thereby achieved. Here, we present our experimental demonstration to such a broadband blueshift tunable metamaterial in the THz regime. This is an important result that gives greater flexibility on multiple switching and modulators using metamaterials, that are tunable to higher (blueshift) and lower (redshift) frequencies on photoexcitation.

The metamaterials were fabricated on commercially available silicon-on-sapphire (SOS) wafers, consisting of a 0.6 μm-thick (100) Si epitaxial layer on top of a 530 μm-thick R-plane sapphire substrate. The intrinsic resistivity of the Si epilayer was not measured, but was specified as >100 Ω cm by the manufacturer. The first step of the fabrication process was the definition of the photosensitive area. This was accomplished by
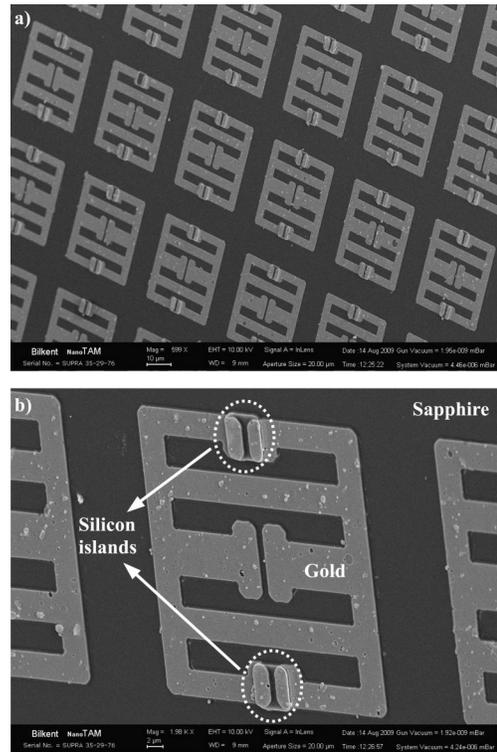

FIG. 2. Optical microscopy images of the fabricated metamaterial device. (a) Large area of the device with an array of hybrid metamaterials; (b) Close view of the unit cell.

photolithographically protecting the two 6×6 μm^2 regions that coincide with the two side gaps of the metallic resonator, and subsequent reactive ion etching (RIE) of the Si epilayer outside the two side gap regions. Next, the photoresist pattern was removed, and a second RIE step was performed on the entire unprotected sample surface to decrease the thickness of the patterned Si layer from 0.6 to 0.2 μm. This resulted in two $6 \times 6 \times 0.2$ μm mesa-shaped Si photosensitive regions per unit cell. During the last step of fabrication, the metallic resonator pattern aligned to the Si photosensitive mesa was defined by photolithography, 150 Å titanium and 2350 Å gold were deposited by E-beam evaporation. Finally, this is followed by removal of unwanted metal. The fabricated sample for measurement is shown in Fig. 2.

For the experimental study of the metamaterial, a powerful THz time domain spectroscopy (TDS) system has been deployed, using an amplified kHz Ti:Sa laser system delivering 35 fs pulses at 800 nm central wavelength and maximum energy of 2.3 mJ per pulse. Part of the initial laser beam with energy equal to 1.3 mJ was focused in ambient air after partial frequency doubling in a beta-barium-borate crystal (50 mm thick) to produce a two-color filament and subsequently, THz radiation [28,29].

For the detection of THz radiation, a small fraction of the initial laser pulse probed the THz-induced birefringence in an electro-optic crystal (1 mm-thick ZnTe) and

monitored the time profile of the THz electric field. The
entire experimental setup was placed inside a purge gas
chamber to avoid water vapor absorption of the THz
radiation.

To study the dynamic response of the metamaterial, an
optical pump beam (800 nm) was used to excite photo-
carriers in the silicon. The sample was placed orthogonally
on the THz beam path and at the focus of the THz beam,
while at 45° to the optical pump beam. At this point, the
THz beam spot's diameter measured about 1.2 mm. The
temporal delay between the optical pump and the THz
beam has been experimentally defined at around 5 ps
(with the photoexcitation occurring before the arrival of
the THz beam). This delay assured a quasisteady state
for the charge carriers of silicon since the lifetime (few
hundreds of nanoseconds) is orders of magnitude longer
than the picoseconds duration of the THz pulse. In addi-
tion, to ensure a uniform photoexcitation and that the
focused optical beam pumps the exact same region of the
sample probed by the THz beam, the pump beam was
expanded to a diameter of 3 mm and a metallic aperture
of 2.2 mm diameter, and placed immediately in front of the
sample. The size of the focused THz beam on the sample
was around 2.2 mm. Any residual pump laser radiation,
which would bring noise in the detection of the THz
electric field, was filtered out by placing a Si wafer
(375 mm thick) just after the sample.

The linearly polarized THz electric field is normally
incident onto the metamaterial sample or the sapphire
substrate, used as reference, and the transmitted THz
electric field pulses are coherently recorded in the time
domain. The frequency-dependent amplitude $t(\omega)$ of the
transmitted THz pulse through the metamaterial is re-
trieved by the division of the sample spectrum with the
reference spectrum $t(\omega) = E_{\text{sample}}(\omega)/E_{\text{reference}}(\omega)$.

The experimental results of the frequency-dependent
response of the studied metamaterial are shown in
Fig. 3(a). With no pump, the normalized transmitted THz
electric field amplitude exhibits a minimum of $t(\omega) \approx$
10% near the resonance at 0.76 THz (black curve). The
off-resonance transmission is around 90%. As the pump
energy flux increases, the resonance initially weakens and
becomes broader and does not shift in frequency. For cases
with a flux value higher than 102.5 μJ/cm^2, the resonance
shows a significant shift to higher frequencies. At the level
with energy flux 294.6 μJ/cm^2, the resonance dip in
the transmission spectrum, $t(\omega) \approx 15\%$, is finally located
at 0.96 THz (red curve), which corresponds to a fairly
broadband blueshift of 26% in the resonance frequency.
Therefore, it is found that the experimental transmission
minima for both resonances at 0.76 THz (no pumping)
and 0.96 THz (photoexcitation power 294.6 μJ/cm^2) are
almost the same. This is a very nice result, which will be
ideal to use for multiple switches and modulators. Our
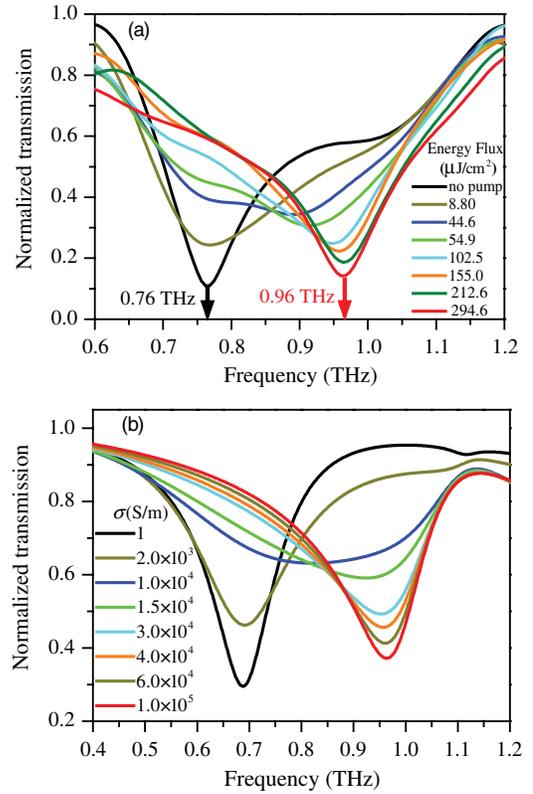experimental approach is compatible with semiconductor

FIG. 3 (color online).   Normalized transmission amplitude of
the THz beam for the metamaterial device as shown in Figs. 1
and 2 (a) Results of experimental measurements as a function of
energy flux of pump beam; (b) Results of simulations as a
function of conductivity of silicon.

technologies and can be used for other applications in
the THz regime.

As a comparison and for understanding our experimen-
tal demonstrations, we present in Fig. 3(b) the results of
numerical simulations performed by the commercial soft-
ware CST Microwave Studio. A single unit cell, as shown
in Fig. 1, is adopted for the simulations with appropriate
boundaries resembling actual conditions in the THz-TDS
experiment. For the metallic parts (gold) of the metamate-
rial resonator, a lossy-metal model is utilized, the conduc-
tivity is $\sigma_{\text{gold}} = 7 \times 10^6$ S/m. The sapphire substrate is
taken as lossless dielectric with $\varepsilon_{\text{Sapphire}} = 10.5$. For the
photoactive silicon parts, we applied a simple conductivity
model, $\varepsilon_{\text{Si}} = 11.7$, and the conductivity, σ_{Si}, is a pending
value chosen to correspond to different pump levels. For
the case without illumination, σ_{Si} was taken to be 1 S/m:
the simulated resonance occurs around 0.69 THz and the
transmission at resonance is around 30%. Following the
increasing pump fluxes, we selected different correspond-
ing values of σ_{Si} to roughly reproduce the experimental
results. The final conductivity of Si was taken as high as
1×10^5 S/m only for obtaining similar transmission be-
havior relative to the no pump case, but it is noticed that
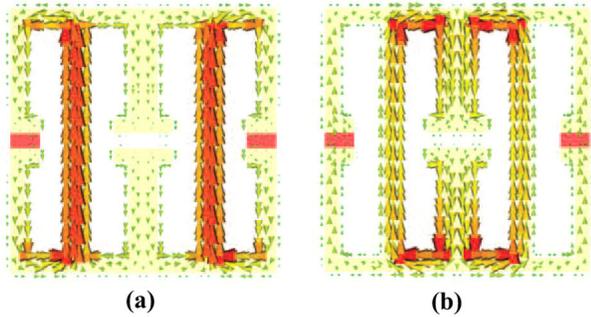actually around $\sigma_{\text{Si}} = 3 \times 10^4$ S/m, the resonance has

FIG. 4 (color online). Distribution of surface current density at resonance frequency. (a) Surface current at $f = 0.7$ THz for $\sigma_{Si} = 1$ S/m (case without pump); (b) Surface current at $f = 0.96$ THz for $\sigma_{Si} = 1 \times 10^5$ S/m (case with highest pump intensity). The red parts within the gaps of two side paths are silicon.

been shifted close to the final frequency 0.96 THz. Therefore, the simulations showed an all-optical blueshift with the tuning range of 40%, compared to 26% in the experiments. Despite of some deviation between the simulation and experimental results, which may be mainly due to imperfections in sample preparation, they are overall in quite good agreement with each other. By investigating the distributions of surface current density at two corresponding resonance frequencies for the cases of no pump and highest pump (shown in Fig. 4), we can intuitively understand the underlying physics for our obtained broadband blueshift tunability: For the case of no pump, the resonator initially works at mode 1 [see the surface current distribution in Fig. 4(a)] where the two side paths are capacitive, but for the high-pump case, the photoinjection in silicon changes the current distribution [see Fig. 4(b)] and pushes the structure to work at mode 2 (with higher resonance frequency), where both the effective inductance and capacitance of the structure decrease in the view of a circuit model. Therefore, our blueshift tunable metamaterial actually works with a photoexcited mode-switching effect, benefiting from the design, which implies two potential resonance states.

In conclusion, we have experimentally demonstrated all-optical broadband blueshift tunability with a metamaterial design in the terahertz regime. The goal was essentially achieved by our proposed photoexcited mode-switching effect, which offers a new path to exploring more designs targeting greater flexibility for practical applications in the range of frequency-agile metamaterials. This work also paves the way for future bi-directional (simultaneously redshift and blueshift) and multiband even cascade switchable devices, which especially benefits various important THz applications in filling the so-called "THz gap."

*stzortz@iesl.forth.gr
†soukoulis@ameslab.gov

[1] C. M. Soukoulis, S. Linden, and M. Wegener, Science **315**, 47 (2007).
[2] V. M. Shalaev, Nat. Photon. **1**, 41 (2007).
[3] J. B. Pendry, Phys. Rev. Lett. **85**, 3966 (2000).
[4] N. Fang, H. Lee, C. Sun, and X. Zhang, Science **308**, 534 (2005).
[5] D. Schurig et al., Science **314**, 977 (2006).
[6] W. Cai, U. K. Chettiar, A. V. Kildishev, and V. M. Shalaev, Nat. Photon. **1**, 224 (2007).
[7] J. Valentine, J. Li, T. Zentgraf, G. Bartal, and X. Zhang, Nature Mater. **8**, 568 (2009).
[8] L. H. Gabrielli, J. Cardenas, C. B. Poitras, and M. Lipson, Nat. Photon. **3**, 461 (2009).
[9] T. J. Yen et al., Science **303**, 1494 (2004).
[10] A. K. Azad, J. Dai, and W. Zhang, Opt. Lett. **31**, 634 (2006).
[11] B. Ferguson and X. C. Zhang, Nature Mater. **1**, 26 (2002).
[12] R. Köhler et al., Nature (London) **417**, 156 (2002).
[13] R. Kersting, G. Strasser, and K. Unterrainer, Electron. Lett. **36**, 1156 (2000).
[14] K. Wang and D. M. Mittleman, Nature (London) **432**, 376 (2004).
[15] T. Kleine-Ostmann, P. Dawson, K. Pierz, G. Hein, and M. Koch, Appl. Phys. Lett. **84**, 3555 (2004).
[16] H. T. Chen et al., Nature (London) **444**, 597 (2006).
[17] W. J. Padilla, A. J. Taylor, C. Highstrete, M. Lee, and R. D. Averitt, Phys. Rev. Lett. **96**, 107401 (2006).
[18] H. T. Chen et al., Opt. Lett. **32**, 1620 (2007).
[19] H. T. Chen et al., Nat. Photon. **3**, 148 (2009).
[20] J. M. Manceau, N. H. Shen, M. Kafesaki, C. M. Soukoulis, and S. Tzortzakis, Appl. Phys. Lett. **96**, 021111 (2010).
[21] N. I. Landy, S. Sajuyigbe, J. J. Mock, D. R. Smith, and W. J. Padilla, Phys. Rev. Lett. **100**, 207402 (2008).
[22] H. Tao et al., Phys. Rev. B **78**, 241103(R) (2008).
[23] B. Wang, T. Koschny, and C. M. Soukoulis, Phys. Rev. B **80**, 033108 (2009).
[24] H. T. Chen et al., Nat. Photon. **2**, 295 (2008).
[25] N. H. Shen et al., Phys. Rev. B **79**, 161102(R) (2009).
[26] D. Schurig, J. J. Mock, and D. R. Smith, Appl. Phys. Lett. **88**, 041109 (2006).
[27] W. J. Padilla et al., Phys. Rev. B **75**, 041102(R) (2007).
[28] K. Y. Kim, A. J. Taylor, J. H. Glownia, and G. Rodriguez, Nat. Photon. **2**, 605 (2008).
[29] A. Couairon and A. Mysyrowicz, Phys. Rep. **441**, 47 (2007).